

# Local Dynamics of the M13 Major Coat Protein in Different Membrane-Mimicking Systems<sup>†</sup>

David Stopar,<sup>‡</sup> Ruud B. Spruijt, Cor J. A. M. Wolfs, and Marcus A. Hemminga\*

Department of Molecular Physics, Agricultural University, Dreijenlaan 3, NL-6703 HA Wageningen, The Netherlands

Received July 18, 1996; Revised Manuscript Received September 20, 1996<sup>®</sup>

**ABSTRACT:** The local environment of the transmembrane and C-terminal domain of M13 major coat protein was probed by site-directed ESR spin labeling when the protein was introduced into three membrane-mimicking systems, DOPC vesicles, sodium cholate micelles, and SDS micelles. For this purpose, we have inserted unique cysteine residues at specific positions in the transmembrane and C-terminal region, using site-directed mutagenesis. Seven viable mutants with reasonable yield were harvested: A25C, V31C, T36C, G38C, T46C, A49C, and S50C. The mutant coat proteins were indistinguishable from wild type M13 coat protein with respect to their conformational and aggregational properties. The ESR data suggest that the amino acid positions 25 and 46 of the coat protein in DOPC vesicles are located close to the membrane–water interface. In this way the lysines at positions 40, 43, and 44 and the phenylalanines at positions 42 and 45 act as hydrophilic and hydrophobic anchors, respectively. The ESR spectra of site specific maleimido spin-labeled mutant coat proteins reconstituted into DOPC vesicles and solubilized in sodium cholate or SDS indicate that the local dynamics of the major coat protein is significantly affected by its structural environment (micellar vs bilayer), location (aqueous vs hydrophobic), and lipid/protein ratio. The detergents SDS and sodium cholate sufficiently well solubilize the major coat protein and largely retain its secondary structure elements. However, the results indicate that they have a poorly defined protein–amphiphilic structure and lipid–water interface as compared to bilayers and thus are not a good substitute for lipid bilayers in biophysical studies.

M13 is a small filamentous bacteriophage that consists of approximately 2700 copies of the gene VIII product, arranged in a helical, cylinder-like coat along a circular single-stranded DNA (Russel, 1991; Marvin et al., 1994). During infection of *Escherichia coli* cells, bacteriophage M13 leaves its major coat protein in the cytoplasmic membrane. Together with newly synthesized coat proteins, it is used for the assembly of the new phage particles at the membrane-bound assembly site (Smilowitz et al., 1972; Russel, 1991; Hemminga et al., 1993). The primary sequence of the coat protein must be such as to allow protein–protein and protein–DNA interactions for the coat protein in the phage and protein–lipid interactions for the membrane-bound M13 coat protein (Hemminga et al., 1992). The relevant part of the primary sequence of M13 coat protein is shown in Figure 1.

The secondary structure of the major coat protein has been extensively studied in micellar model systems by various NMR<sup>1</sup> techniques (Henry et al., 1987; Henry and Sykes, 1992; McDonnell et al., 1993; Van de Ven et al., 1993). It is, however, interesting to note that there exists a remarkable

discrepancy between the predicted transmembrane domain and the NMR assigned transmembrane helix of the protein in micellar systems (see Figure 1). Various hydropathy calculations predict different hydrophobic domain stretches ranging from Glu20 to Thr46 depending on the hydropathy scale and subsequent calculational strategies (for an evaluation, see Turner & Weiner, 1993). Especially, the membrane–water interface at the C-terminus of the major coat protein is poorly defined, mainly because of the presence of three positively charged lysine residues, which are intercalated between apolar aromatic phenylalanine residues (Turner & Weiner, 1993). Most hydropathy calculations suggest that Phe42 and Phe45 are located in an unfavorable hydrophilic environment. This is unlikely, since aromatic amino acids are often found near the lipid–water interface, where they anchor the protein in the membrane (Deisenhofer et al., 1985; Weiss et al., 1991). The NMR data, on the other hand, suggest a firm  $\alpha$ -helix between Tyr24 and Phe45 in SDS micelles leaving only the last four to five amino acids in the C-terminus unstructured (Henry et al., 1987; Henry & Sykes, 1992; McDonnell et al., 1993; Van de Ven et al., 1993). From binding studies, it is also known that when a peptide associates with a membrane interface, the probability of secondary structure formation increases drastically, because the interface restricts the degrees of freedom of the peptide (White & Wimley, 1994). Therefore, the predicted transmembrane domain in the C-terminal part of the major coat protein may be shifted up to Thr46. When a transbilayer phosphate to phosphate distance of 4.5 nm is taken into account, the membrane could easily accommodate more than 20 amino acid residues (Altenbach et al., 1994).

<sup>†</sup> This research was supported by Slovenian Ministry of Science and Technology.

\* Author to whom correspondence should be addressed at the Department of Molecular Physics, Agricultural University, P.O. Box 8128, 6700 ET Wageningen, The Netherlands.

<sup>‡</sup> Permanent address: University of Ljubljana, Biotechnical Faculty, Vecna pot 111, 61000 Ljubljana, Slovenia.

<sup>®</sup> Abstract published in *Advance ACS Abstracts*, November 1, 1996.

<sup>1</sup> Abbreviations: CD, circular dichroism; CL, cardiolipin; DTNB, 5,5'-dithiobis(2-nitrobenzoic acid); DOPC, 1,2-dioleoyl-*sn*-glycero-3-phosphocholine; DOPG, 1,2-dioleoyl-*sn*-glycero-3-phosphoglycerol; ESR, electron spin resonance; HPSEC, high-performance size exclusion chromatography; L/P, lipid to protein molar ratio; NMR, nuclear magnetic resonance; SDS, sodium dodecyl sulfate; EDTA, ethylenediaminetetraacetic acid.

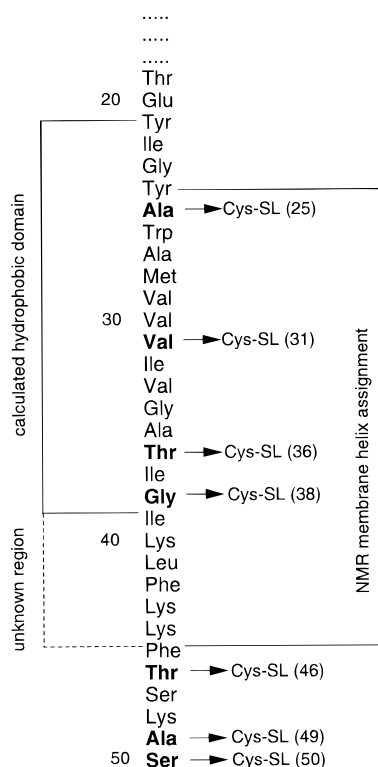


FIGURE 1: Part of primary structure of M13 gene VIII product (major coat protein) with calculated hydrophobic domain, unknown region (dotted line) (Makino et al., 1975) and helix assignment as found from NMR (Chamberlain & Webster, 1978; Brotherus et al., 1981; Cross & Opella, 1985). Bold-type amino acid residues are mutated to cysteine residues and used for ESR spin labeling. SL indicates the spin label 3-maleimidoproxyl that is used in the spin-labeling experiments.

Two widely accepted membrane model systems for biophysical studies are detergent micelles and lipid bilayers. Lipid bilayers are more appropriate to mimic the typical structure of a biological membrane, due to its well-characterized structure. Most of the structural determination on the major coat protein, however, has been carried out in micellar systems, mainly in SDS (Cross & Opella, 1980; Henry et al., 1987; Henry & Sykes, 1992; McDonnell et al., 1993; Van de Ven et al., 1993). Therefore, it is interesting to compare the conformational state of the protein in lipids with the well-described state of the protein in micellar systems. For this reason, a site-directed spin-labeling approach for membrane-embedded M13 coat protein is followed in this paper. A similar approach for the major coat protein has been followed recently by Khan and Deber (1995) and Wolkers et al. (unpublished experiments).

Analysis of the ESR line shape of the spin-labeled mutants provides direct information about the motional properties of the spin label that reflect the local structure of the protein. Since M13 major coat protein contains no cysteine residues, we have introduced unique cysteine residues at selected positions along the protein primary structure. For this substitution the following strategy was chosen: (1) mutant bacteriophages must be viable; this ensures that the mutation causes a minimal perturbation of the native secondary structure and is thus a good representative of the wild type coat protein; (2) mutations should be located in different topological domains of the coat protein, i.e., membrane-embedded positions as compared to positions in the aqueous phase.

In this paper ESR experiments have been carried out on spin-labeled major coat protein mutants, reconstituted into phospholipid bilayers of DOPC, and solubilized in sodium cholate and SDS micelles. Our data suggest that amino acids 25 and 46 of the coat protein are located close to the membrane–water interface. The local dynamics of the spin-labeled protein is significantly affected by its structure and local environment, and there are marked differences in local dynamics between DOPC and SDS. These results agree with a parallel study carried out by Spruijt et al. (1996), in which cysteine mutants of the M13 coat protein were employed for fluorescent labeling and reactivity studies with DTNB.

## MATERIALS AND METHODS

**Chemicals.** DOPC, DOPG, CL, sodium cholate, and DTNB (Ellman's reagent) were obtained from Sigma. SDS was purchased from Merck. Mutagenic oligonucleotides were synthesized by Pharmacia Biotech. The spin label 3-maleimido proxyl was obtained from Aldrich Chemical Co. Poly(A) and oligophosphates 15 and 25 in length were purchased from Pharmacia Biotech and Sigma, respectively.

**Preparation of Cysteine-Containing Coat Protein Mutants.** Single cysteine-containing major coat protein mutants were prepared as described previously (Spruijt et al., 1996). Mutant bacteriophages were grown to milligram quantities as described previously for wild type bacteriophage M13 (Spruijt et al., 1989). The primary structure of the mutant coat proteins was deduced from the DNA sequence as obtained from automated sequencing.

**Solubilization, Labeling, and Purification of the Major Coat Protein in SDS and Sodium Cholate Micelles.** The SDS-isolated coat proteins were spin labeled with 3-maleimidoproxyl at a spin label to protein ratio of 3/1 (mol/mol) directly after disruption of the bacteriophage in 175 mM SDS, 150 mM NaCl, 10 mM Tris, and 0.2 mM EDTA, pH 7.0. The labeling reaction was carried out at 37 °C and was stopped after 60 min by adding an excess of cysteine to the reaction mixture. The mixture was then applied to a Sephacryl S-300 column (3.7 × 65 cm) and eluted with 25 mM SDS, 150 mM NaCl, 10 mM Tris-HCl, and 0.2 mM EDTA, pH 8.0 to separate viral DNA and unbound spin label from the spin-labeled coat protein. Fractions with an absorbancy ratio  $A_{280}/A_{260}$  greater than 1.5 were collected. Prior to the ESR measurements samples were concentrated by an Amicon stirring cell. The cholate-isolated coat proteins were prepared as described above with SDS replaced by 25 mM sodium cholate. Before storage at 4 °C, sodium cholate was added up to 50 mM to prevent possible protein aggregation. The amount of spin label bound to the coat protein after spin labeling was calculated after determination of the free thiol groups using DTNB.

**Reconstitution of the Major Coat Protein in the Lipid Bilayers.** From the desired amount of lipid solution, chloroform was evaporated with nitrogen gas and subsequently dried under vacuum for at least 2 h. The lipids were solubilized in a 50 mM sodium cholate buffer (150 mM NaCl, 10 mM Tris-HCl, and 0.2 mM EDTA, pH 8.0) by sonication for 1 min. The spin-labeled protein in 50 mM sodium cholate buffer and phospholipids were mixed to obtain the desired L/P (mol/mol) ratio. To avoid spin–spin interactions the mutant coat protein was diluted 10 times with unlabeled wild type protein. Reconstitution was carried out

by cholate dialyses at room temperature against a 100-fold excess buffer (150 mM NaCl, 10 mM Tris-HCl, and 0.2 mM EDTA, pH 8.0) for a total of 48 h, the buffer being changed every 12 h. After dialysis, the samples were concentrated for ESR purposes as described by Sanders et al. (1991). To obtain multilamellar vesicles the samples were freeze-dried and resuspended with distilled water. For the purpose of poly(A) and oligophosphate binding studies, unilamellar vesicles with the desired L/P (mol/mol) ratio were prepared by sonication and dialysis as described above and concentrated using ultracentrifugation (Beckman, 3 h at 45 000 rpm). These samples were not freeze-dried. The aggregational and conformational states of samples in the lipid bilayers as well as in SDS and sodium cholate micelles were checked using HPSEC (Spruijt et al., 1989). The L/P ratios and homogeneity in L/P ratios were determined after sample preparation as described previously (Spruijt et al., 1989). CD measurements were performed on a Jobin-Yvon Dichograph Mark V in the wavelength range 190–290 nm as described by Sanders et al. (1993).

**Oligonucleotide and Oligophosphate Binding.** For titration with poly(A) and oligophosphates, unilamellar vesicles were prepared as described above. The use of unilamellar vesicles ensures that all the added poly(A) and oligophosphates is able to bind to the reconstituted coat protein in the vesicles. In the binding experiments, the desired amount of freshly prepared poly(A) or oligophosphate stock solution was added to a constant amount of coat protein reconstituted in vesicles.

**ESR Studies.** Samples containing the labeled major coat protein solubilized in 50 mM sodium cholate buffer or 25 mM SDS buffer and reconstituted in unilamellar or multilamellar lipid vesicles were filled up to 5 mm with sample in 100  $\mu$ L glass capillaries and were accommodated within standard 4 mm diameter quartz tubes. ESR measurements were performed on a Bruker ESP 300E ESR spectrometer equipped with a 4103 TM microwave cavity at room temperature. The ESR settings were 6.38 mW microwave power, 0.1 mT modulation amplitude, 40 ms time constant, 160 s scan time, 10 mT scan width, and 348.5 mT center field. Up to 200 spectra were accumulated to improve the signal to noise ratio.

## RESULTS

Using the strategy described in the introduction, viable mutants with X-Cys substitutions at amino acid positions 25, 31, 33, 36, 38, 46, 47, 49, and 50 were harvested (Spruijt et al., 1996). For the purpose of our study, seven bacteriophage mutants with reasonable yield for biophysical studies (5–25% of wild type yield) were selected and grown to milligram quantities: A25C, V31C, T36C, G38C, T46C, A49C, and S50C. DNA sequence analysis indicated that, in addition to the single cysteine residue incorporated at the desired position, the mutants A25C, T36C, G38C, T46C, and A49C have a second spontaneous mutation at amino acid 27: A27S. Mutant V31C has a unique cysteine mutation, while the S50C mutant has a second mutation N12D, which converts this coat protein into a closely related fd major coat protein. An additional check carried out with the DTNB reaction confirms the insertion of only one cysteine residue per protein monomer. The efficiency of spin labeling of major coat protein with 3-maleimidopropyl spin label in 100 mM sodium cholate buffer was 50–95% for various mutants.

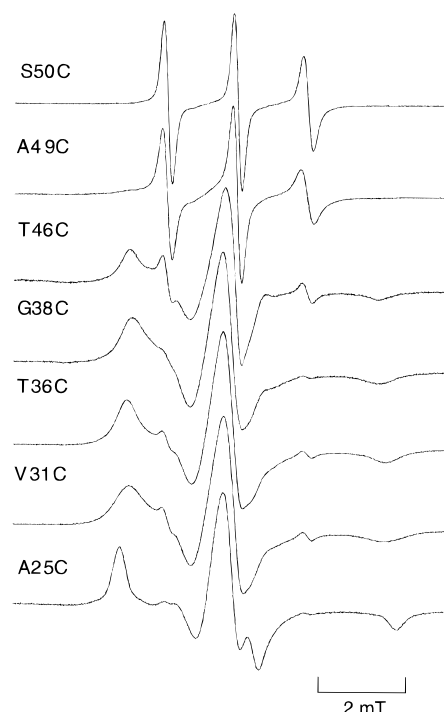


FIGURE 2: ESR spectra of 3-maleimidopropyl site-specific spin-labeled M13 mutant coat proteins at various positions, reconstituted in DOPC multilamellar vesicles at L/P 35 in 150 mM NaCl, 10 mM Tris, and 0.2 mM EDTA at room temperature. Spectral line heights are normalized to each other.

This percentage was generally lower for the SH groups inside the predicted transmembrane domain. The labeling efficiency for the mutants reconstituted in SDS micelles was 10–20% lower as compared to that when sodium cholate micelles were used.

The spin-labeled mutant proteins reconstituted in DOPC vesicles were compared with the wild type M13 coat protein with respect to their homogeneity in L/P ratio, conformation, and aggregation properties. Sucrose density gradient centrifugation showed a single band, indicating that the samples were homogeneous in L/P ratio. HPSEC elution profiles showed that the spin-labeled mutant coat proteins did not differ from the wild type proteins with respect to the aggregational properties. The CD spectra of the spin-labeled mutant proteins in sodium cholate micelles were comparable to those of unlabeled wild type M13 coat protein under the same conditions. Within experimental error the overall secondary structure of the mutant proteins is retained and indicative for an  $\alpha$ -helical form (Spruijt & Hemminga, 1991; Sanders et al., 1993). This finding, together with the relatively high viability of the mutants, also indicates that the second non-cysteine compensating mutation (A27S or N12D) does not significantly influence the conformation of the mutant coat protein.

The ESR spectra of the various spin-labeled coat protein mutants reconstituted into phospholipid bilayers of DOPC and solubilized in sodium cholate and SDS are shown in Figures 2–4, respectively. To characterize the ESR spectra, the rotational correlation time  $\tau_c$  is used for the spin labels at positions 49 and 50 (see Table 1) that are characteristic for a fast isotropic motion. For the other spin-labeled mutant coat proteins, which have a powder-like appearance, the outer hyperfine splitting  $2A_{zz}$  is used as a relative measure of spin label mobility (see Figure 5).

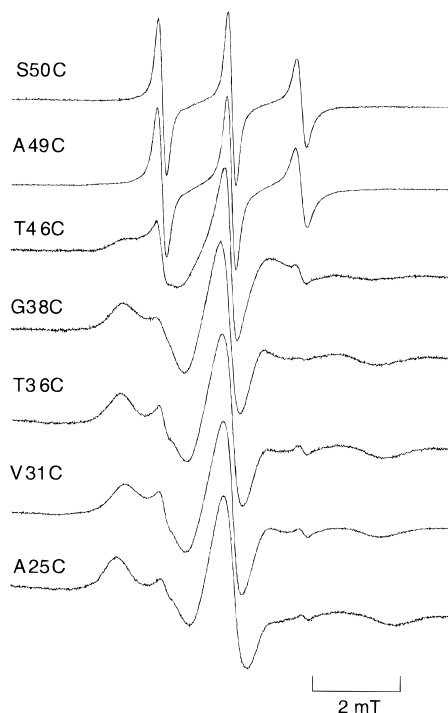


FIGURE 3: ESR spectra of 3-maleimidoproxyl site-specific spin-labeled M13 mutant coat proteins at various positions solubilized in 50 mM sodium cholate, 150 mM NaCl, 10 mM Tris, and 0.2 mM EDTA at room temperature. Spectral line heights are normalized to each other.

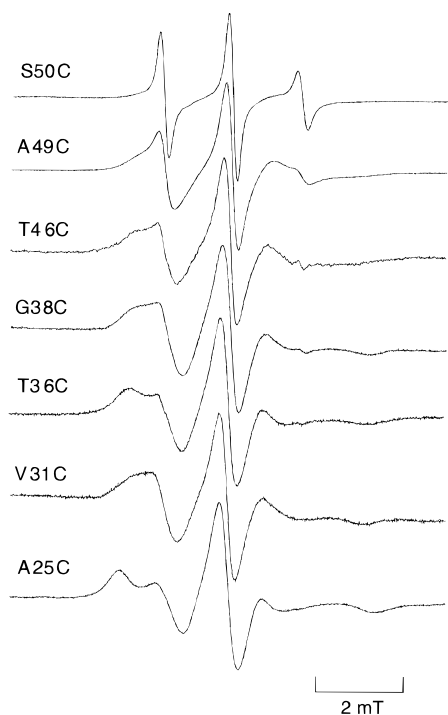


FIGURE 4: ESR spectra of 3-maleimidoproxyl site-specific spin-labeled M13 mutant coat proteins at various positions dissolved in 25 mM SDS, 150 mM NaCl, 10 mM Tris, and 0.2 mM EDTA at room temperature. Spectral line heights are normalized to each other.

The ESR spectra of spin-labeled mutants that are solubilized in sodium cholate follow the same tendency as found in DOPC. However, the spectra are substantially more broadened, especially for the spin labels at positions 25 and 46. The ESR spectra of spin-labeled mutants that are solubilized in SDS micelles have a strongly reduced outer

Table 1: Rotational Correlation Times  $\tau_c$  of 3-Maleimidoproxyl Labeled Mutant Major Coat Protein A49C and S50C at Room Temperature in Various Model Systems

$\tau_c$ (ns) <sup>a</sup>	DOPC	sodium cholate	SDS
A49C	0.88	0.55	≈10
S50C	0.40	0.41	0.70

<sup>a</sup> The  $\tau_c$  values are calculated from the spectra in Figures 2–4 according to Marsh (1981).

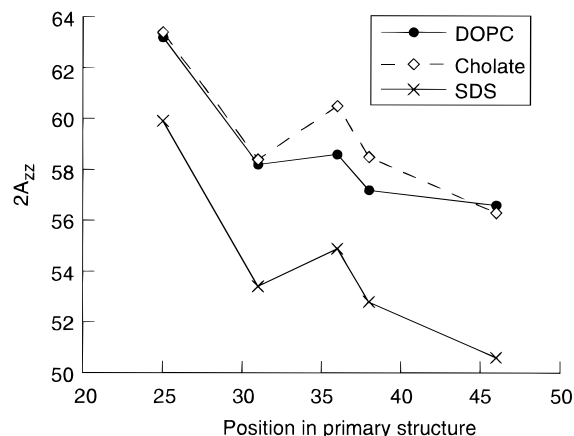


FIGURE 5: The outer splitting in millitesla for the spin label ESR spectra in Figures 2–4 at the various positions.

hyperfine splitting (Figure 5). It is interesting to note that the spin labels at positions 49 and 50, when reconstituted in DOPC and sodium cholate, are characteristic for a fast isotropic motion (see also Table 1), but are significantly reduced in mobility when solubilized in SDS micelles. In all model systems studied for the spin label at position 36, a slightly increased outer hyperfine splitting is observed, indicating a higher local order parameter. This effect can be explained by the presence of the bulky side chains of Val33 and Ile39 one helix turn up and down position 36, respectively. This indicates that the local motion of spin labels attached to proteins can monitor the presence of amino acids, although this effect is small. In all model systems studied the spin label at position 25 has a distinct powder line shape.

In the ESR spectra in Figures 2–4, a small additional spectral contribution with sometimes a large (5.7 mT) or a small (1.6 mT) hyperfine splitting can be observed, depending on the position of labeling. Such spectral components are also observed in samples of spin-labeled wild type M13 coat protein (data not shown) and can be attributed to spin-labeled terminal amino groups and  $\epsilon$ -amino groups of lysines of the coat protein. No further attempts were made to subtract these components from the spectra.

To monitor the effect of the L/P ratio on the ESR spectra, the spin-labeled mutant coat proteins G38C, T46C, and A49C were reconstituted in DOPC vesicles. The rotational correlation time  $\tau_c$  was used to characterize the rotational mobility for the spin label at position 49. The outer hyperfine splitting  $2A_{zz}$  was used for the spin labels at positions 38 and 46. Independent of the topological location of the spin label (i.e., membrane or aqueous), the same L/P dependence is obtained with a sharp change at an L/P ratio of about 15 (see Figure 6). The observed decrease of the spin label motion at low L/P ratios can be explained by protein–protein interactions (Sanders et al., 1992). Therefore, all further

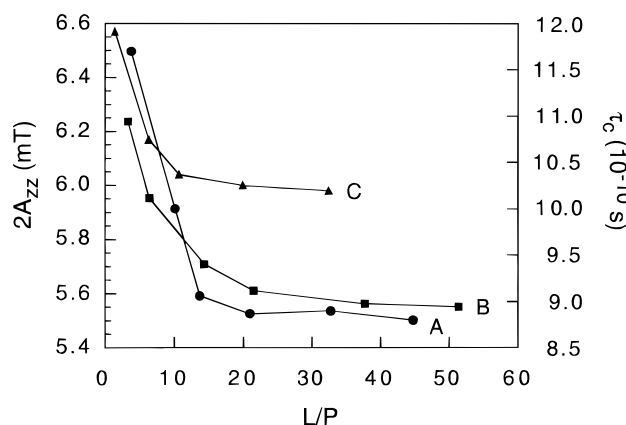


FIGURE 6: Variation of  $\tau_c$  (right vertical scale) of maleimido spin label attached at position 49 (A) and  $2A_{zz}$  (left vertical scale) of the spin label attached at positions 46 (B) and 38 (C) as a function of the L/P ratio.

studies were performed at L/P 20 or higher to avoid direct protein–protein interactions.

Upon reconstitution of the mutant coat proteins G38C, T46C, and A49C, which are expected to be close to the phospholipid head group region and located in the lysine-rich domain of the protein, into phospholipids (L/P > 20) with increasing negative charge [that is, DOPC/DOPG (80/20 mol/mol), DOPC/CL (80/20 mol/mol), DOPG, and DOPG/CL (80/20 mol/mol)], there are only small differences in the ESR line shape (data not shown). The mobility of the spin label at position 49 increases (up to 3%), while the outer splitting of the spin label at position 38 decreases (up to 2%) as compared to DOPC. The spin label at position 46 is not affected by a change of phospholipid system. These results indicate that the positive charges of the coat protein are already effectively neutralized by the zwitterionic DOPC.

Two spin-labeled mutant coat proteins, T46C and A49C, with the spin label located in the lysine-rich C-terminal domain of the protein, which is responsible for DNA binding in the virus particle, were also examined for possible binding effects of negatively charged molecules on their mobility. Spin-labeled mutant coat proteins reconstituted in unilamellar DOPC vesicles (L/P > 20) were titrated with oligophosphates and poly(A). Over a large range of nucleotide to protein ratios 0–60 and NaCl concentrations 15–150 mM, no effects on the spin label mobility could be detected (data not shown).

## DISCUSSION

Site-directed ESR spin labeling is used in this paper to probe the local dynamics of the M13 coat protein reconstituted in three membrane-mimicking systems. Seven mutants with relatively good yield were used, covering the hydrophobic and the C-terminal part of the protein from amino acid positions 25 to 50. With respect to the membrane-bound properties, the analysis of the structural and aggregational properties of the mutant coat proteins incorporated in phospholipid systems shows that the mutant proteins are indistinguishable from the wild type M13 coat protein. Thus, site-specific mutagenesis results in functional mutant coat proteins with cysteines at locations representative of different topological domains in the major coat protein and a yield high enough to make them suitable for biophysical studies.

**M13 Coat Protein in Phospholipid Bilayers.** The ESR spectra of site-specific spin-labeled mutant coat proteins

reconstituted in DOPC vesicles (Figure 2) are indicative for a large range of molecular motions sensed by the maleimido spin label. The 3-maleimidopropyl spin label, which has a relatively small size due to its short linker close to the protein backbone, seems to represent well the different local environments of the protein. The high isotropic flexibility of the spin labels at positions 49 and 50 is in agreement with the absence of a rigid helical structure in this part of the C-terminal region as found by NMR spectroscopy of M13 coat protein solubilized in SDS (Henry & Sykes, 1992; McDonnell et al., 1993; Van de Ven et al., 1993). The isotropic hyperfine splitting is 1.58 mT, which is characteristic for a hydrophilic environment of the two spin labels (Fretten et al., 1980). As is shown in Figure 6, the spin label at position 49 is sensing the presence of other protein molecules in DOPC bilayers at low L/P ratios. Although this effect is small (the decrease of  $\tau_c$  is about 20%), this indicates that the mainly segmental motion of the spin label in the terminal protein part is influenced by adjacent termini. However, the packing of the C-termini of M13 coat protein at low L/P is not so dense that the motion of the spin label is completely blocked.

The spectrum of the spin label attached to a cysteine at positions 31, 36, and 38 is typical for an immobilized spin label with an outer hyperfine splitting  $2A_{zz}$  of about 5.8 mT (see Figure 5). This is, however, significantly less than for a rigid limit nitroxide spectrum ( $2A_{zz} \approx 6.40$  mT), suggesting that some relatively fast, probably anisotropic, motion is taking place. This observation is further confirmed by the large widths of the low- and high-field peaks in the spectrum. The line shapes are very similar to the spectrum of a phosphatidylcholine C-5 spin label in phospholipid systems with an outer splitting  $2A_{zz}$  of 5.86 mT and an order parameter of 0.8 (Griffith & Jost, 1976). This similarity indicates that the anisotropic motion is taking place around the principal  $z$ -axis of the maleimido spin label. As has been discussed previously for the analysis of ESR and saturation transfer ESR spectra of maleimido spin labeled coat protein of the plant virus cowpea chlorotic mottle virus, such an anisotropic motion arises from a local motion of the maleimido spin label about the long axis of the molecule (Vriend et al., 1984; Hemminga & Faber, 1986). Therefore, we interpret the ESR spectrum as a fast wobbling motion of the maleimido spin label at the cysteine within a cone. From the estimated order parameter ( $\approx 0.8$ ) it can be calculated that the total cone angle is about  $40^\circ$ .

The ESR spectra in Figure 2 are recorded at an L/P ratio of 35. As is illustrated in Figure 6, at this L/P ratio, direct protein–protein contacts are expected to give only a small contribution to the reduced motion of the spin label at positions 25, 31, 36, and 38 as compared to the spin label at position 49. Based on transmembrane helix prediction methods, it is well established that residues Ala25 to Gly38 of M13 coat protein are embedded in the hydrophobic part of lipid systems (Kyte & Doolittle, 1982; Turner & Weiner, 1993). Thus, the immobilization of the spin label at positions 25 to 38 is in agreement with this concept, because there is a strong increase in local viscosity when going from the aqueous phase to the hydrophobic part of the lipid system. In addition, the presence of anisotropic motion is a strong indication for a reduced local flexibility provided by the presence of a helical protein structure.

It is interesting to note that, although position 46 is close to position 49 and predicted to be in the hydrophilic environment, the line shape of the spin label attached to a cysteine at position 46 is characteristic for an intermediate slow motion ( $\tau_c \approx 10^{-8}$ – $10^{-9}$  s). Clearly, there is a mobility gradient in the C-terminal part of the coat protein reconstituted in DOPC vesicles with a dramatic decrease of local viscosity from positions 49 to 46. This can be explained by assuming that the transmembrane domain of the coat protein coincides with the transmembrane helix as assigned by NMR. It was discussed previously in a parallel study using the accessibility of different fluorescence quenchers in fluorescence labeling studies on the major coat protein mutants (Spruijt et al., 1996) that position 46 is located close to the membrane interface. The spin label data are consistent with this conclusion.

A consequence of this finding is that Lys40, Lys43, and Lys44 are buried in the membrane. It is known that, due to its long apolar side chain, a lysine can have its  $\alpha$ -carbon in the membrane interior, while its positively charged  $\epsilon$ -amino group is able to interact with the negatively charged phosphate groups of the phospholipids (Tanford & Reynolds, 1976; Hemminga et al., 1992). This is not unlikely, because of a high molar excess of phosphates in the phospholipid head groups. Since Lys40 is buried deeply in the membrane, distance measurements were carried out on a molecular model of the major coat protein, assuming an  $\alpha$ -helical structure from Tyr24 to Thr46 using the computer program Insight II (Biosym Technologies) on a Silicon Graphics. The bond lengths were kept fixed, while the bond angle between the  $\alpha$ ,  $\beta$ , and  $\gamma$  carbons of the lysines was allowed to change, without changing the overall structure of the model. These studies indicate that the  $\epsilon$ -amino group of Lys40 is able to reach the phosphate groups of the head group region located around Thr46. The  $\epsilon$ -amino groups of the side chains of Lys43 and Lys44 can reach the head group region more easily, or could even stick out into the aqueous phase. An interaction with the head group phosphates could also be possible for Lys48, which is present in the aqueous phase, but our results cannot confirm this possibility.

The absence of any structural or motional effect of (oligo)-phosphates and poly(A) titration on reconstituted spin-labeled M13 coat protein in DOPC is an additional argument for lysines interacting with lipid phosphates. We cannot completely exclude weak electrostatic interactions of the C-terminal lysines with DNA in a membrane-bound form, however, they do not manifest themselves in change of the local motion of the protein. This supports the idea that lysines are buried in the lipid head group region, where they can interact with the large molar excess of proximal phosphates.

Another interesting feature of the C-terminal part of M13 coat protein is the presence of two aromatic residues Phe42 and Phe45. It has been described in the literature that aromatic residues play a key role in maintaining a stabile association of the proteins in a membrane environment (Deisenhofer et al., 1985; Henderson et al., 1990; Weiss et al., 1991). Phe45, which is next to the 46 position in the phospholipid head group region, is also in an unfavorable environment, unless its aromatic side chain is sticking backward into the membrane interior. Molecular modeling, as described above, shows that the aromatic side chain is probably located in the region of the glycerol moieties of

the phospholipids. By combining these conclusions, it turns out that the C-terminal protein part is very well anchored, because the lysine and phenylalanine residues serve as hydrophilic and hydrophobic anchors, respectively. In the case that the protein tends to move up or down along a normal to the membrane surface, either the phenylalanine or the lysine residues would be in an unfavorable environment.

The proposed extension of the transmembrane domain disagrees with the hydropathy profiles (Makino et al., 1975; Kyte & Doolittle, 1982), which predict that Thr46 is outside the membrane (Figure 1). This discrepancy arises mainly because the hydropathy scales recognize entire lysine residues to be external to the membrane (Turner & Weiner, 1993).

In comparison with the other ESR line shapes, the spectrum of the spin label at the position 25 is remarkable. In previous work of our group, it has been discussed that this spectrum arises from an anisotropic motion of the maleimido spin label about the principal  $z$ -axis of the nitroxide  $g$ -factor and hyperfine tensors with a high order parameter ( $S \approx 1$ ) (Wolkers et al., unpublished experiments). This high value implies that the spin label experiences a strong squeezing effect by its local environment, which reduces the amplitude of its wobbling motion. This squeezing effect is suggested to arise from a turn structure in the coat protein from Glu20 to Gly23 in the membrane–water interface at the N-terminal domain of the major coat protein.

**M13 Coat Protein in Detergents.** Detergents have been used often to solubilize M13 coat protein for biophysical studies. In fact, all high-resolution NMR work has been carried out with SDS-solubilized coat protein. To make a comparison of the state of the protein in bilayers as compared to well-described detergent systems, spin-labeled coat protein mutants were also solubilized in sodium cholate and SDS. Although the spectra in cholate are following the same tendency as in DOPC, they are more broadened (see Figure 3). The broadening effect is especially strong for the spin label at positions 25 and 46. This broadening is probably due to an increased molecular motion of the protein, as compared to the DOPC bilayer system. This gives rise to an incomplete averaging of the solid state powder components in the line shape. When the protein was solubilized in SDS micelles (see Figure 4), a strong reduction of the outer splittings (Figure 5) is observed for the spin label at positions 25–46, indicating an even more increased molecular motion and reduced order parameter.

In cholate, the molecular motion of the spin label at the C-terminal positions 49 and 50 is only slightly affected as compared to the bilayer system (see Table 1), suggesting a comparable state of the C-terminal part in both systems. However, in SDS the motion of the spin labels at positions 49 and 50 is significantly reduced, suggesting a strongly reduced motion of the C-terminal region. This indicates that SDS is covering the whole C-terminal part of the coat protein as well as the hydrophobic region, without a well-defined boundary as found in a bilayer. This is not surprising when the solubilizing properties of the SDS are taken into account. SDS is a strong amphiphilic molecule, and it is also well-known that for a variety of proteins there is a constant binding ratio of the SDS to the protein on a gram to gram basis (Helenius & Simons, 1975). Clearly, this nonspecific covering effect is not present with sodium cholate as a detergent molecule, because the spin labels at positions

49 and 50 are not affected by the presence of the sodium cholate and are located in an aqueous environment. Cholate is a flat hydrophobic molecule and, as can be deduced from the ESR spectra, is preferentially bound to the hydrophobic parts of the protein. In this respect, sodium cholate better mimics the typical nature of a membrane structure as compared to SDS micelles.

The distinct powder line shape for the spin label at position 25 in all model systems studied (Figures 2–4) is remarkable. It has been suggested that the line shape in DOPC bilayers arises from a reduction of the spin label motion by a specific  $\beta$ -turn structure formed between residues 21 and 23 at the membrane–water interface (Wolkers et al., unpublished experiments). Due to this turn the amphiphilic N-terminal helix and the transmembrane helix become almost perpendicular to each other, and according to this model, the spin label is squeezed between the two helices. It can be seen from the ESR spectra in the different model systems that this effect is most pronounced in DOPC, indicating that the bilayer structure stabilizes an L-shaped conformation. The special property of the spin label at position 25 is also seen in the high value of the outer hyperfine splitting (see Figure 5).

**Biological Relevance and Conclusions.** Our data suggest an extension of the predicted transmembrane domain of M13 coat protein toward the C-terminus up to Thr46 in DOPC lipid bilayers, leaving the side chains of Lys40, Lys43, Lys44, and Phe42 and Phe45 at the water–membrane interface. This provides a very good anchoring mechanism for the coat protein, because the lysine and phenylalanine residues serve as hydrophilic and hydrophobic anchors, respectively. The effective neutralization of lysine  $\epsilon$ -NH<sub>2</sub> groups by the high molar excess of the phosphates in proximal head groups may also provide a protection of the lysines in the *E. coli* cytoplasm during virus replication. Although there might be some weak electrostatic interactions between the reconstituted protein and DNA or other negatively charged molecules in the aqueous phase, they will generally exist as independent species. This implies a mechanism in which the coat protein can interact with the DNA only when it is released from the phospholipids. An additional hydrophobic interaction between the major coat proteins could stabilize such a protein–DNA complex in a process which is mediated by the host and virus protein assembly machinery (Russel, 1991).

From the data presented in this paper it can be seen that the local dynamics of the major coat protein is significantly affected by its structural environment (micellar vs bilayer), location (aqueous vs hydrophobic), and L/P ratio. Although the detergents SDS and sodium cholate sufficiently well solubilize the coat protein and largely retain its secondary structure elements, they have a poorly defined protein–amphiphilic structure and lipid–water interface as compared to bilayers and thus are not a good substitute for lipid bilayers in biophysical studies.

## REFERENCES

- Altenbach, C., Greenhalgh, D. A., Khorana, H. G., & Hubbell, W. L. (1994) *Proc. Natl. Acad. Sci. U.S.A.* 91, 1667–1671.
- Brotherus, J. R., Griffith, O. H., Brotherus, M. O., Jost, P. C., Silvius, J. R., & Hokin, L. E. (1981) *Biochemistry* 20, 5261–5267.
- Chamberlain, B. K., & Webster, R. E. (1978) *J. Bacteriol.* 135, 883–887.
- Cross, T. A., & Opella, S. J. (1980) *Biochem. Biophys. Res. Commun.* 92, 478–484.
- Cross, T. A., & Opella, S. J. (1985) *J. Mol. Biol.* 182, 367–381.
- Deisenhofer, J., Epp, O., Miki, K., Huber, R., & Michel, H. (1985) *Nature* 318, 618–624.
- Fretten, P., Morris, S. J., Watts, A., & Marsh, D. (1980) *Biochim. Biophys. Acta* 598, 247–259.
- Griffith, H. O., & Jost, P. C. (1976) in *Spin Labeling. Theory and applications* (Berliner, L. J., Ed.) pp 453–523, Academic Press, New York, San Francisco, London.
- Helenius, A., & Simons, K. (1975) *Biochim. Biophys. Acta* 415, 29–79.
- Hemminga, M. A., & Faber, A. J. (1986) *J. Magn. Reson.* 66, 1–8.
- Hemminga, M. A., Sanders, J. C., & Spruijt, R. B. (1992) in *Progress in Lipid Research* (Sprecher, H., Ed.) Vol. 31, pp 301–333, Pergamon Press, Oxford.
- Hemminga, M. A., Sanders, J. C., Wolfs, C. J. A. M., & Spruijt, R. B. (1993) in *Protein-Lipid Interactions* (Watts, A., Ed.) New Comprehensive Biochemistry 25, pp 191–212, Elsevier, Amsterdam.
- Henderson, R., Baldwin, J. M., Ceska, T. A., Zemlin, F., Beckmann, E., & Downing, K. H. (1990) *J. Mol. Biol.* 213, 899–929.
- Henry, G. D., & Sykes, B. D. (1992) *Biochemistry* 31, 5284–5297.
- Henry, G. D., Weiner, J. H., & Sykes, B. D. (1987) *Biochemistry* 26, 3626–3634.
- Khan, A. R., & Deber, C. M. (1995) *Biochem. Biophys. Res. Commun.* 206, 230–237.
- Kyte, J., & Doolittle, R. F. (1982) *J. Mol. Biol.* 157, 105–132.
- Makino, S., Woolford, J. L., Jr., Tanford, C., & Webster, R. E. (1975) *J. Biol. Chem.* 250, 4327–4332.
- Marsh, D. (1981) in *Membrane Spectroscopy* (Grell, E., Ed.) pp 51–142, Springer-Verlag, Berlin.
- Marvin, D. A., Hale, R. D., Nave, C., & Citterich, M. H. (1994) *J. Mol. Biol.* 235, 260–286.
- McDonnell, P. A., Shon, K., Kim, Y., & Opella, S. J. (1993) *J. Mol. Biol.* 233, 447–463.
- Russel, M. (1991) *Mol. Microbiol.* 5, 1607–1613.
- Sanders, J. C., Poile, T. W., Spruijt, R. B., van Nuland, N. A. J., Watts, A., & Hemminga, M. A. (1991) *Biochim. Biophys. Acta* 1066, 102–108.
- Sanders, J. C., Ottaviani, M. F., van Hoek, A., Visser, A. J. W. G., & Hemminga, M. A. (1992) *Eur. Biophys. J.* 20, 305–311.
- Sanders, J. C., Haris, P. I., Chapman, D., Otto, C., & Hemminga, M. A. (1993) *Biochemistry* 32, 12446–12454.
- Smilowitz, H., Carson, J., & Robbins, P. W. (1972) *J. Supramol. Struct.* 1, 8–18.
- Spruijt, R. B., & Hemminga, M. A. (1991) *Biochemistry* 30, 11147–11154.
- Spruijt, R. B., Wolfs, C. J. A. M., & Hemminga, M. A. (1989) *Biochemistry* 28, 9158–9165.
- Spruijt, R. B., Wolfs, C. J. A. M., Verver, J. W. G., & Hemminga, M. A. (1996) *Biochemistry* 35, 10383–10391.
- Tanford, C., & Reynolds, J. A. (1976) *Biochim. Biophys. Acta* 457, 133–170.
- Turner, R. J., & Weiner, J. H. (1993) *Biochim. Biophys. Acta* 1202, 161–168.
- Van de Ven, F. J. M., Van Os, J. W. M., Aelen, J. M. A., Wymenga, S. S., Remerowski, M. L., Konings, R. N. H., & Hilbers, C. W. (1993) *Biochemistry* 32, 8322–8328.
- Vriend, G., Schilthuis, J. G., Verduin, B. J. M., & Hemminga, M. A. (1984) *J. Magn. Reson.* 58, 421–427.
- Weiss, M. S., Abele, U., Weckesser, J., Welte, W., Schiltz, E., & Schulz, G. E. (1991) *Science* 254, 1627–1630.
- White, S. H., & Wimley, W. C. (1994) *Curr. Opin. Struct. Biol.* 4, 79–86.